Frascati Physics Series Vol. 73 (2022)
LFC22: Strong interactions from QCD to new strong dynamics at LHC and Future Colliders
August 29 - September 2, 2022

INITIAL-STATE QED RADIATION AT NLL ACCURACY FOR FUTURE ELECTRON-POSITRON COLLIDERS

Giovanni Stagnitto
Physik-Institut, Universität Zürich, Winterthurerstrasse 190, CH-8057 Zürich, Switzerland

Abstract

We present state-of-the-art results for the QED Parton Distribution Functions (PDFs), which have been recently pushed up to next-to-leading logarithmic (NLL) accuracy. In particular, in this contribution, we will focus on a simple process as a toy model to explore the impact of NLL PDFs and the dependence on the renormalisation and factorisation scheme.

It is not unreasonable to assume that the future of high-energy physics will involve an e^+e^- collider. It is time for the theoretical community to start thinking about how to enlarge the legacy of LEP. The techniques and the calculations developed for LEP need to be revisited to keep up with the astonishing projected experimental error on measurements at future colliders. The relative error on several electroweak observables will reach 0.01% and possibly be even smaller.

The typical cross section relevant to e^+e^- collisions is in principle entirely computable as a perturbative series in the QED coupling constant α. However, calculations of processes in QED always feature large contributions stemming from photon collinear emissions in the initial state (initial state radiation, ISR). These contributions appear as logarithms to some power of some hard physical scale Q over the mass of the electron m_e, $L = \log^k(Q^2/m_e^2)$:

$$d\sigma_{e^+e^-} = \alpha^b \sum_{n=0}^{\infty} \alpha^n \left(c_0^{(n)} + c_1^{(n)} L + \ldots + c_n^{(n)} L^n \right) , \tag{1}$$

with b the power of α in the Born process. These logarithmic terms can be numerically large, preventing the perturbative series from being well behaved.

It is fortunate that such $\log^k(Q^2/m^2)$ terms are universal, hence they can be taken into account to all orders in α by a process-independent resummation procedure. With the *collinear factorisation* approach,

the physical cross section is written by means of a factorisation formula that recalls the standard QCD factorization formula at hadron colliders:

$$d\sigma_{e^+e^-} = \sum_{ij} \int dz_+ dz_- \, \Gamma_{i/e^+}(z_+, \mu^2, m_e^2) \, \Gamma_{j/e^-}(z_-, \mu^2, m_e^2) \, d\hat{\sigma}_{ij}(z_+, z_-, Q^2, \mu^2) + \mathcal{O}\left(\frac{m_e^2}{Q^2}\right) . \quad (2)$$

Let us describe the various terms present in this equation: $d\sigma_{e^+e^-}$ is the *particle-level* cross section, computed with massive electrons; $d\hat{\sigma}_{ij}$ is a *parton-level* cross section, understood to be computed with massless electrons, which does not contain any logarithmic term, and is expected to be well-behaved order by order in perturbation theory; $z_\pm$ are the longitudinal momentum fractions carried by the partons w.r.t. their mother particle; $\Gamma_{i/e^\pm}$ are the Parton Distribution Functions (PDFs) of the electron or the positron, a name that originates from the analogy of Eq. 2 with its QCD counterpart. PDFs are universal and resum to all order the collinear logarithms due ISR. Note that the nature of the parton entering the short-distance cross section can coincide with that of the incoming particle e.g. $(i, j) = (e^+, e^-)$, or it can differ e.g. $(i, j) = (\gamma, e^-), (e^-, e^-), \ldots$. Moreover, as in QCD, a suitable factorisation scheme must be introduced (e.g. $\overline{\text{MS}}$) to regulate the zero-mass divergences in the parton-level cross section and a factorization scale μ^2 appears both in the $\Gamma_{i/e^\pm}$ and in $d\hat{\sigma}_{ij}$.

At variance with hadronic PDFs, QED PDFs are entirely calculable with perturbative techniques. In the following, we will mostly focus on the PDFs relevant to an incoming unpolarised electron particle, $\Gamma_{i/e^-} \equiv \Gamma_i$; the PDFs of an incoming positron are trivially related by charge conjugation. We will refer to Γ_{e^-} as electron PDF, and to Γ_γ as photon PDF. At the initial scale $\mu_0^2 \simeq m_e^2$, the leading order initial condition is a trivial $\Gamma_{e^-}(z, \mu_0^2) = \delta(1 - z)$. The PDF at the final scale μ^2 can be obtained by means of QED DGLAP evolution equations [1, 2, 3, 4]. At leading logarithmic (LL) accuracy i.e. the resummation of the dominant tower of $(\alpha L)^k$ terms, analytical expressions have been known for a long time [2, 3, 5, 6]:

$$\Gamma_{e^-}^{\text{LL}}(z, \mu^2) = \frac{\exp\left[(3/4 - \gamma_E)\eta\right]}{\Gamma(1 + \eta)} \eta (1 - z)^{-1+\eta} - \frac{1}{2}\eta(1 + z) + \mathcal{O}(\alpha^2) , \quad \eta = \frac{\alpha}{\pi} L . \quad (3)$$

Such LL analytical expressions are built out of an additive matching between a recursive solution up to some order in α, typically $\mathcal{O}(\alpha^3)$, and an all-order α solution valid in the region $z \to 1$. Note that with Q of the order of a few hundred GeV's one obtains $\eta \sim 0.05$. Therefore, because of the $(1 - z)^{-1+\eta}$ factor, the PDF is very peaked towards $z = 1$, where it diverges with an integrable singularity. In general, such a peculiar structure of the PDFs requires a suitable re-parameterization of the phase-space [7] when numerically performing the convolution in Eq. 2.

In view of high-energy future colliders and the need for precise predictions, LL accuracy for QED PDFs is certainly insufficient. Moreover, theoretical systematics are not well defined in a LL-accurate picture. For instance, the value of α in Eq. 3 is entirely arbitrary at LL: whether α runs or not, or more generally in which renormalisation scheme α is defined, are questions that arise only at higher orders. To improve on the LL result, one can calculate individual higher powers of $\alpha^l L^k$ by means of fixed-order calculations (see e.g. [8] and references therein) or extend the resummed result to next-to-leading logarithmic (NLL) accuracy i.e. resumming also the tower of $\alpha(\alpha L)^k$ terms. We will focus on the latter.

In Ref. [9], the electron, positron, and photon PDFs of the unpolarised electron have been calculated at NLL accuracy in the $\overline{\text{MS}}$ factorisation and renormalisation scheme. The PDFs have been derived by solving the DGLAP equations both numerically and analytically, by using as initial conditions for the evolution the ones derived in Ref. [10]. In Ref. [11], these results have been improved in several directions: first, with a DGLAP evolution featuring multiple fermion families (leptons and quarks) in

a variable flavour number scheme i.e. by properly including the respective mass thresholds; second, by taking into account an alternative factorisation scheme, the Δ scheme [12], where the NLO initial condition are maximally simplified; third, by considering two alternative renormalisation schemes, $\alpha(m_Z)$ and G_μ schemes (where α is fixed).

NLL PDFs ready for phenomenology can be obtained with the public code EMELA, available here:

`https://github.com/gstagnit/eMELA`

Such a code supersedes the one developed in Ref. [9] (EPDF), that was limited to the evolution with a single lepton in the $\overline{\rm MS}$ renormalisation and factorisation schemes. EMELA is a standalone code, and can be linked to any external program. Since a runtime evaluation of the numerical solution is likely too slow for phenomenological applications, the possibility is given to the user to output the PDFs as grids compliant with the LHAPDF [13] format, that can be employed at a later stage. Moreover, regardless of whether the numerical solution is computed at runtime or read from the grids, EMELA always switches to the analytical solution for $z \to 1$. EMELA can also provide one with PDFs with beamstrahlung effects, according to the procedure presented in Ref. [7].

In Ref. [11], EMELA has been linked to MADGRAPH5_AMC@NLO [14, 15] in order to reach NLL accuracy for the PDFs and NLO accuracy (in the full electroweak theory) for the short-distance cross section, and obtain first NLL+NLO predictions for physical observables at lepton colliders. While MADGRAPH5_AMC@NLO is widely used in the context of LHC simulations, it can also be employed for lepton collisions. Indeed, many results for leptonic collisions were already provided in Ref. [14], including NLO-QCD corrections but limited to the case of a strictly fixed centre-of-mass energy. The extension to the case with QED ISR and beamstrahlung has been documented in Ref. [7], whereas Ref. [11] describes the inclusion of NLO EW corrections to the short distance cross section, allowing for the computation of NLL+NLO observables after linking to EMELA.

In order to investigate the effect of NLL PDFs, here we focus on a toy model process,

$$e^+e^- \to q\bar{q}(\gamma)\,, \tag{4}$$

with a final state photon only present in the real-emission NLO contribution. In Eq. 4, q is a massless fermion of charge e_q, and in the corresponding short-distance cross sections we retain only the contributions proportional to e_q^2 (this limits the real and virtual radiation to the initial state, and thus the process is effectively equivalent to that for the production of a heavy neutral object of variable mass). Note that this is the process already used in Ref. [10] for the determination of the initial conditions for the electron PDFs. The process under consideration is simple enough to be easy to calculate (indeed its simple analytical cross sections have been used as a cross-check of the corresponding automated computation carried out by MG5_AMC), but interesting enough to be able to draw some physical considerations.

We calculate the particle-level (parton-level) cross section as differential in τ ($\hat{\tau}$), defined as:

$$\tau = \frac{M^2_{q\bar{q}}}{s}\,, \quad \hat{\tau} = \frac{M^2_{q\bar{q}}}{\hat{s}} = \frac{\tau}{z_+ z_-}\,, \tag{5}$$

with $M^2_{q\bar{q}}$ the invariant mass squared of the pair of final state quarks. Eq. 2 can be rewritten as

$$\frac{d\sigma}{d\tau} = \int_0^1 {\rm d}z_+ {\rm d}z_- d\hat{\tau}\, \Gamma_{e^-}(z_+,\mu_F^2)\, \Gamma_{e^-}(z_-,\mu_F^2)\, \frac{d\hat{\sigma}}{d\hat{\tau}}(\hat{\tau},\mu_F^2)\, \delta(z_+ z_- \hat{\tau} - \tau)\,, \tag{6}$$

with the parton-level cross section given by the sum of the LO and the NLO contributions,

$$\frac{d\hat{\sigma}}{d\hat{\tau}} = \frac{d\hat{\sigma}^{[0]}}{d\hat{\tau}} + \frac{\alpha}{2\pi}\frac{d\hat{\sigma}^{[1]}}{d\hat{\tau}}\,. \tag{7}$$

The LO contribution is trivially given by

$$\frac{d\hat{\sigma}^{[0]}}{d\hat{\tau}} = B(\hat{s})\,\delta(1-\hat{\tau})\,, \quad B(\hat{s}) = \frac{4\pi\alpha^2}{3\hat{s}}\,. \tag{8}$$

In full generality, the NLO contribution is given by

$$\begin{aligned}\frac{d\hat{\sigma}^{[1]}}{d\hat{\tau}} = B(\hat{s})\frac{1}{\hat{\tau}}\Bigg[&2\left(\frac{1+\hat{\tau}^2}{(1-\hat{\tau})_+} + \frac{3}{2}\delta(1-\hat{\tau})\right)\log\frac{\hat{s}}{\mu_F^2} - 2K_F(\hat{\tau}) + 2(2\pi)K_R\delta(1-\hat{\tau}) \\ &+ 4(1+\hat{\tau}^2)\left(\frac{\log(1-\hat{\tau})}{1-\hat{\tau}}\right)_+ + \delta(1-\hat{\tau})\left(-\frac{92}{9} + \frac{2}{3}\pi^2 + \frac{4}{3}\log\frac{\hat{s}}{\mu_R^2}\right)\Bigg]\,.\end{aligned} \tag{9}$$

The term proportional to K_F is related to the change of factorisation scheme, with the factor of 2 due to the fact that there are two incoming legs. In the $\overline{\text{MS}}$ factorisation scheme, $K_F^{\overline{\text{MS}}}(z) = 0$, whereas in the e.g. Δ scheme we have

$$K_F^{\Delta}(z) = \left[\frac{1+z^2}{1-z}\left(2\log(1-z)+1\right)\right]_+\,. \tag{10}$$

The term proportional to K_R is related to the change of factorisation scheme, with the factor of 2 due to the power of α in Eq. 8. In the $\overline{\text{MS}}$ renormalisation scheme, $K_R^{\overline{\text{MS}}}(z) = 0$, whereas in the e.g. $\alpha(m_Z)$ scheme with a single active lepton, by neglecting the presence of thresholds and the W-boson contribution to the running of α, we have

$$K_R^{\alpha(m_Z)} = \frac{1}{3\pi}\log\frac{\mu_R^2}{m_Z^2} + \frac{5}{9\pi}\,. \tag{11}$$

More involved expressions in presence of multiple fermion families (leptons and quarks) by properly including the respective mass thresholds can be easily obtained with the results presented in Sec. 4 of Ref. [11].

In the following, we will focus on the cumulative cross section defined as

$$\sigma(\tau_{\min}) = \int d\sigma\,\Theta\left(\tau_{\min} \le \frac{M_{q\bar{q}}^2}{s}\right) = \int_0^1 \mathrm{d}z_+\mathrm{d}z_-\,\Gamma_{e^-}(z_+)\,\Gamma_{e^-}(z_-)\,\Theta\left(\frac{\tau_{\min}}{z_+z_-} < 1\right)\int_{\tau_{\min}/(z_+z_-)}^1 d\hat{\tau}\,\frac{d\hat{\sigma}}{d\hat{\tau}}\,, \tag{12}$$

with the integral of parton-level NLO contribution given by

$$\begin{aligned}\frac{1}{B(\hat{s})}\int_c^1 d\hat{\tau}\,\frac{d\hat{\sigma}^{[1]}}{d\hat{\tau}} = &-\frac{56}{9} - 4c + \frac{4}{3}\log\frac{\hat{s}}{\mu_R^2} + (4\pi)K_R - 2\int_c^1 d\hat{\tau}\,\frac{K_F(\hat{\tau})}{\hat{\tau}} \\ &- 4(1-c)\log(1-c) + 4\log^2(1-c) + 4\mathrm{Li}_2(c) \\ &+ \log\frac{\hat{s}}{\mu_F^2}\left(1 + 2c + 4\log(1-c) - 2\log c\right)\,.\end{aligned} \tag{13}$$

The integral of the K_F function in the Δ scheme reads

$$\int_c^1 d\hat{\tau}\,\frac{K_F^{\Delta}(\hat{\tau})}{\hat{\tau}} = 2\mathrm{Li}_2(c) - c + 2\log^2(1-c) + 2c\log(1-c) - \log(c) - \frac{\pi^2}{3} - 1\,. \tag{14}$$

We present numerical results for the the cumulative cross section Eq. 12 for the toy model process at $\sqrt{s} = \mu_R = \mu_F = 500$ GeV. Ratios of $\sigma(\tau_{\min})$ for different settings of the PDFs are shown in Fig. 1 and Fig. 2 as a function of $\tau_{\min}$. We find qualitatively similar results in the range $\sqrt{s} \in [50, 500]$ GeV. The region close to $\tau_{\min} = 1$ has to be taken with a grain of salt because it features unresummed purely soft logs.

In Fig. 1 on the left, we show the dependence of the cumulative cross section on the adopted factorisation scheme. Such a dependence is of the order of 10^{-4}–10^{-3}, to be considered as a systematic error associated to the calculation. Note that the NLL electron PDF largely differs ($\mathcal{O}(1)$) between the $\overline{\text{MS}}$ and the Δ scheme, with the NLL electron PDF in the Δ scheme closer to the LL value [11]. Hence we can conclude that there are large cancellations between the PDFs and the short-distance cross section in the $\overline{\text{MS}}$ scheme, cancellations which are absent for the Δ scheme. Such benefial cancellations in the Δ scheme are also evident in the cumulative short-distance cross section, Eq. 13: when inserting Eq. 14 into Eq. 13, we see that the $\log^2(1-c)$ term cancels entirely.

In Fig. 1 on the right, we show the dependence of the cumulative cross section on the adopted renormalisation scheme. By comparing with Fig. 1 on the left, we see that the renormalisation scheme dependence mostly leads to a normalisation effect, and it is significantly larger than the factorisation scheme one. The choice of the renormalisation scheme should be regarded as an informed choice rather than a systematic of the calculation.

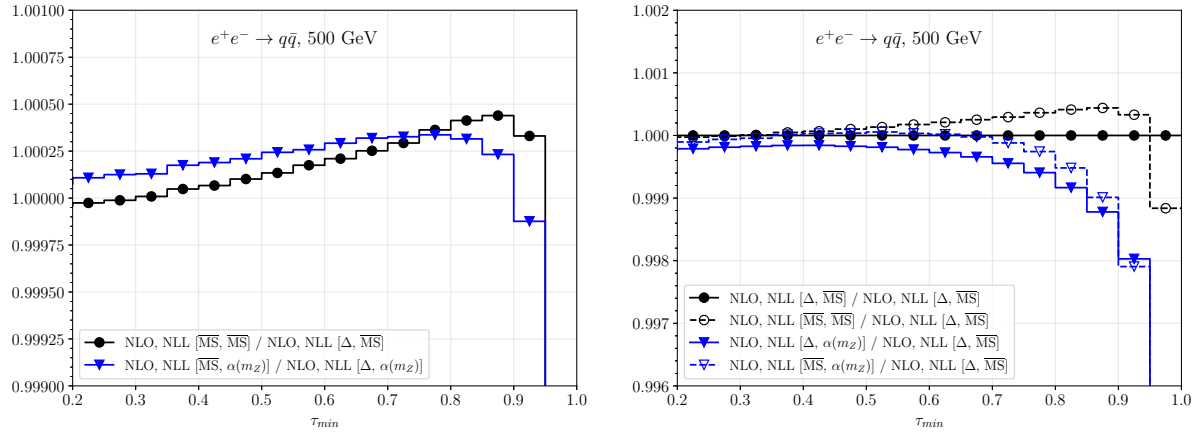

Figure 1: Dependence of the cumulative cross section Eq. 12 for the toy model process on factorisation and renormalisation schemes at $\sqrt{s} = \mu_R = \mu_F = 500$ GeV . Several choices of factorisation and renormalisation schemes for the PDFs are shown. The notation adopted in the legends of the plots is: {accuracy of short-distance cross section}, {accuracy of PDF} [{factorisation scheme}, {renormalisation scheme}]. The accuracy of the short-distance cross section is always NLO.

In Fig. 2, the impact of NLL vs. LL PDFs is shown for three different choices of renormalisation schemes. It is clear that the corrections due to next-to-leading logarithms follow a non-trivial pattern, impossible to account in some universal manner. Hence, NLL-accurate PDFs are phenomenologically important for precision studies.

Note that, despite its semplicity, the toy model process behaves similary (w.r.t. ISR effects) to the other $2 \to 2$ processes considered in Ref. [11]. We refer the interested reader to Refs. [10, 9, 7, 12, 11] for additional details about predictions at high-energy e^+e^- colliders within collinear factorisation and the usage of NLL PDFs. As a final remark, we would like to stress that moving towards NLL is important not only to improve on the accuracy of our predictions, but also needed for an assessment of sources of theoretical uncertainties.

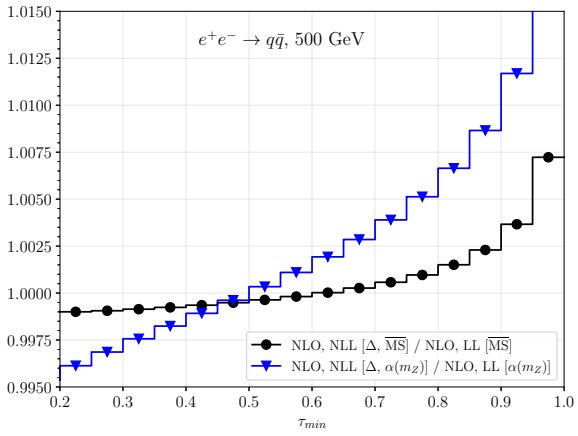

Figure 2: Impact of next-to-leading logarithmic terms in the PDFs. The notation adopted is as in Fig. 1.

1 Acknowledgements

The work presented in this contribution benefited from collaboration with V. Bertone, M. Cacciari, S. Frixione, M. Zaro and X. Zhao, to whom I am grateful. This work has received funding from the Swiss National Science Foundation (SNF) under contract 200020-204200.

References

1. G. Altarelli *et al*, *Nucl. Phys. B* **126** 298 (1977).
2. V.N. Gribov *et al*, *Sov. J. Nucl. Phys.* **15** 438 (1972).
3. L.N. Lipatov, *Yad. Fiz.* **20** 181 (1974).
4. Y.L. Dokshitzer, *Sov. Phys. JETP* **46** 641 (1977).
5. M. Skrzypek *et al*, *Z. Phys. C* **49** 577 (1991).
6. M. Cacciari *et al*, *Europhys. Lett.* **17** 123 (1992).
7. S. Frixione *et al*, `2108.10261`.
8. J. Blümlein *et al*, *Mod. Phys. Lett. A* **37** 2230004 (2022) [`2202.08476`].
9. V. Bertone *et al*, *JHEP* **03** 135 (2020) [`1911.12040`].
10. S. Frixione, *JHEP* **11** 158 (2019) [`1909.03886`].
11. V. Bertone *et al*, *JHEP* **10** 089 (2022) [`2207.03265`].
12. S. Frixione, *JHEP* **07** 180 (2021) [`2105.06688`].
13. A. Buckley *et al*, *Eur. Phys. J. C* **75** 132 (2015) [`1412.7420`].
14. J. Alwall *et al*, *JHEP* **07** 079 (2014) [`1405.0301`].
15. R. Frederix *et al*, *JHEP* **07** 185 (2018) [`1804.10017`].